Supplementary information of

Elastic Constants of Biological Filamentous Colloids: Estimation and Implications on Nematic and Cholesteric Tactoid Morphologies

Massimo Bagnani[1], Paride Azzari[1], Cristiano De Michele[2], Mario Arcari[1] and Raffaele Mezzenga[1,3]*

[1]ETH Zurich, Department of Health Sciences and Technology, Schmelzbergstrasse 9, LFO E23 Zurich 8092, Switzerland.

[2]"Sapienza" Universita' di Roma, Dipartimento di Fisica, P.le A. Moro 2, 00185 Roma, Italy

[3]ETH Zurich, Department of Materials, Wolfgang-Pauli-Strasse 10, Zurich 8093, Switzerland.

*Correspondence to: raffaele.mezzenga@hest.ethz.ch

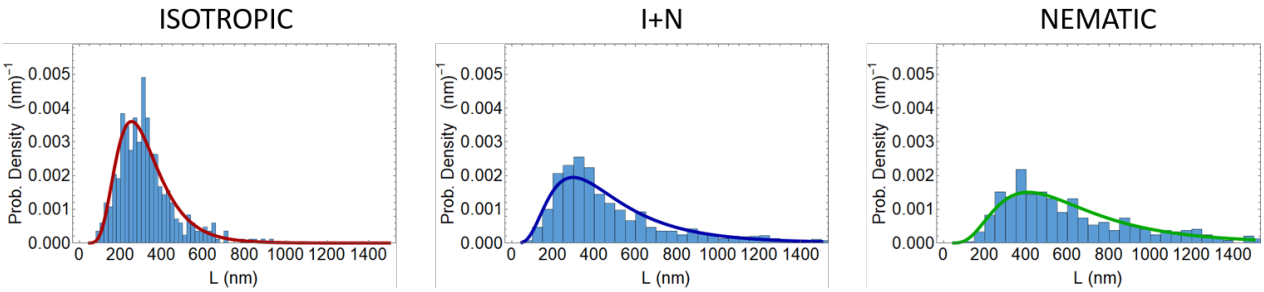

Figure S1 *Length distributions of amyloid fibrils. The histograms show the length distributions of amyloid in the isotropic phase (left), in the isotropic-nematic mixture (center) and in the nematic phase (right). The solid lines represent the log-normal fits.*

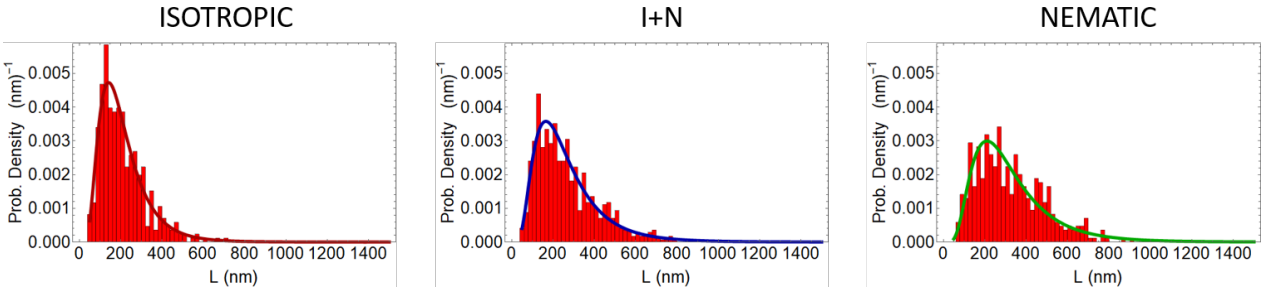

Figure S2 *Length distributions of sulfated cellulose nanocrystals. The histograms show the*

length distributions of SCNCid in the isotropic phase (left), in the isotropic-nematic mixture (center) and in the nematic phase (right). The solid lines represent the log-normal fits.

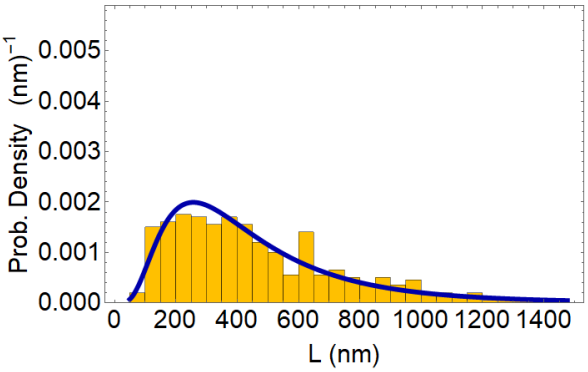

Figure S3 *Length distributions of carboxylated cellulose nanocrystals. The histograms show the length distributions of CCNC in in the isotropic-nematic mixture. The solid line represents the log-normal fit.*

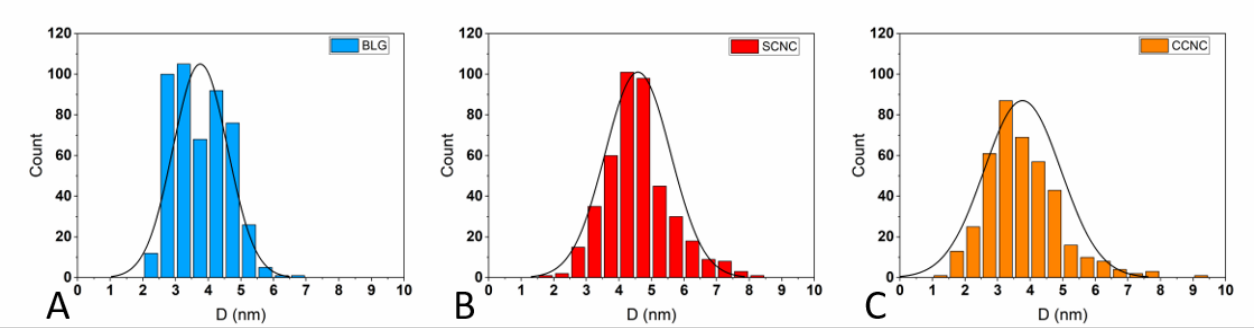

Figure S4 *Height distributions of BLG amyloid fibrils (A), SCNC (B) and CCNC (C). The histograms show the height distributions for the three systems extracted from AFM analysis. The solid lines represent the normal distribution fit. The average height, corresponding to the rods diameter (D), resulted 3.75±0.83 nm for BLG, 4.6±1.00 nm for SCNC and 3.75±1.18 nm for CCNC.*

Effective diameter

In order to evaluate the elastic constant behavior of the three system studied, the effect of electrostatic interactions on the effective diameter of the rods is investigated. The effective diameter proposed by Onsager, when taking into account the changes become:

$$D_{eff} = D + k^{-1}(lnA + C + ln2 - \frac{1}{2})$$

where D is the diameter of the rod, k^{-1} the Debye length, C the Euler's constant ($C = 0.577$) and A, for weakly charged rod in anisotropic phase, is given by eq. (5.1) in ref.[1] and is equal to:

$$A = \frac{8\pi Q e^{-kD}}{\upsilon_{eff} k^3 D^2 K_1^2(\frac{1}{2}kD)}$$

Where Q is the Bjerrum length (0.71 nm), K_1 the modified Bessel function υ_{eff} the linear charge density.

For BLG we have a linear charge density of ~0.43 e/nm , at ionic strength of 13.4 mmol/L , Debye 2.6 nm[2]. For CCNC we have from ionic strength of ~0.56 mmol/L (Gustav acs nano), surface charge 0.038 e/nm^2 , lin. Charge 0.19 e/nm, Debye Length 12.9 nm[3]. For SCNC we have an ionic strenght 4.2 mM/L, lin. Charge 0.66 e/nm, Debye length 4.7 nm[4].

Persistence length measurements

Beta-lactoglobulin amyloid fibrils are characterized by a persistence length of 1.98 μm[5] . For the other two systems SCNC and CCNC, AFM measurments were performed and persistence length values extracted from MS end-to-end distance $\langle R^2 \rangle$ plots in fig. S2. In case of SCNC and CCNC the persistence length estimated was 3.3 and 1.3 μm respectively. Due to the crystalline nature of cellulose rods, it is intuitive to have persistence length higher compared to amyloid, such as SCNC. However, CCNC seems show more flexible behavior due to the numerous kinks formed during sample preparation[6].

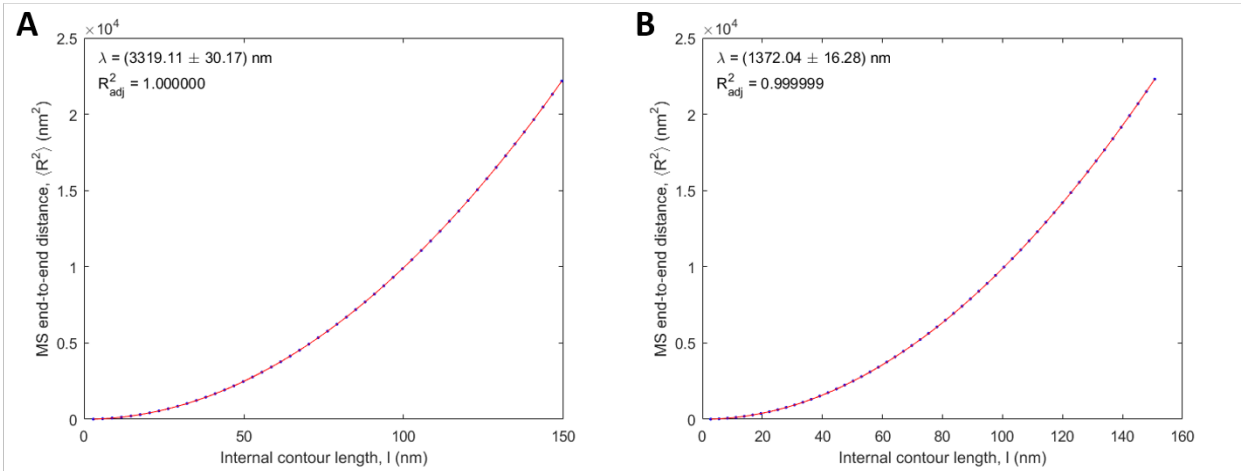

Figure S5 *Persistence length measurements. The blue dots are experimental points and the red line is the fit. The persistence length of SCNC and CCNC measurements obtained by AFM analysis are plotted in panel (A) and (B) respectively.*

System	D (nm)	D_{eff} (nm)	<L> (nm)	L_p (nm)	L_p/<L>
BLG	3.75±0.8	5.5±0.8	652±400	1980	3.0±1.8
S CNC	4.6±1.0	15.7±1.0	325±168	3319	10.2±5.3
C CNC	3.75±1.1	20.0±1.1	465±281	1370	2.9±1.8

Table S1 *Summary table of the characteristic parameters for the three different systems extracted from AFM analysis of 486, 426 and 400 particles for BLG, SCNC and CCNC respectively.*

Molecular Theory

Following the theory proposed in Ref.[1], the elastic contributions F_{el} to the free energy of a nematic/cholesteric phase formed by a polydisperse mixture of fibrils can be expressed as a functional of the contour length distribution of fibrils $\nu(L)$, where L is the length of a fibril. The contour length distribution obeys the normalization condition $\int_0^\infty \nu(L) = 1$. By truncating the Taylor expansion of F_{el} with respect to the nematic director displacements, we can write:

$$\frac{F_{el}}{V} = \frac{1}{2} K_1 {q_1}^2 + \frac{1}{2} K_2 {q_2}^2 + \frac{1}{2} K_3 {q_3}^2 \quad (1)$$

where q_1, q_2 and q_3 are the wavelengths of the distortion associated to splay (K_1), twist (K_2) and bend elastic constants, respectively.

Following Ref.[7], segments (fibrils) shorter than L_0 are considered as rigid, while those longer than or equal to L_0 are decomposed into effective rigid segments of length L_0, so that the elastic constants can be written as follows:

$$K_i = \frac{k_B T\, \eta(\Phi) A^2}{2} \left[\int_0^{L_0} \int_0^{L_0} dL\, dL'\, \nu(L)\nu(L')\, \overline{v}_{ii}(L, L') + 2 \int_0^{L_0} \int_{L_0}^{\infty} dL\, dL'\, \nu(L)\nu(L')\, \frac{L'}{L_0}\, \overline{v}_{ii}(L, L_0) + \int_{L_0}^{\infty} \int_{L_0}^{\infty} dL\, dL'\, \nu(L)\nu(L')\, \frac{L\, L'}{L_0^2}\, \overline{v}_{ii}(L_0, L_0) \right] \quad (2)$$

where $A = \frac{c_m}{\mu_0\, L_c}$ with c_m mass concentration of fibrils, μ_0 the mass of a fibril per unit length and L_c the average length of the fibrils (the values of these parameters used in the calculations are reported in Table 1), T is the temperature, $\overline{v}_{ii}$ are the generalized excluded volumes between two fibrils 1 and 2 of length L and L' respectively[2] and $\eta(\Phi)$ is the Parsons−Lee which is introduced to account for higher order terms in the virial expansion. Here, $\Phi = \xi\, \phi$, with ϕ the volume fraction of fibrils is an effective volume fraction and ξ a scaling factor which should be intended to an adjustable parameter which is introduced to account for electrostatic repulsion. In our calculations we set $\xi = 2.7$, so that the value of the splay elastic constant (K_1) of betalactoglobuline fibrils is roughly in line with the other estimates discussed in the main text (i.e. $K_1 \approx 1\ pN$).

The generalized excluded volumes $\overline{v}_{ii}$ can be expressed as follows:

$$\overline{v}_{ii}(L, L', \alpha_N) = -\int \left(\vec{R}_{12}^{i}\right)^2 e_{12}^{LL'}\left(\vec{R}_{12}, \vec{\Omega}_1, \vec{\Omega}_2\right) \left(\vec{u}_1 \cdot \hat{X}\right) \left(\vec{u}_2 \cdot \hat{X}\right) \dot{f}_O(x)\big|_{x=\vec{u}_1\cdot\hat{Z}} \dot{f}_O(x)\big|_{x=\vec{u}_2\cdot\hat{Z}}$$

$$d\vec{R}_{12} d\vec{\Omega}_1 d\vec{\Omega}_2 \tag{3}$$

where $\vec{u}_i$ is the unit vector parallel to the axis of the fibril i (with $i = 1,2$) which is treated as an hard cylinder , $\vec{\Omega}_i$ are the Euler angles that define its orientation in the laboratory frame, $\vec{R}_{12}^{i}$ is a cartesian component of vecrtor $\vec{R}_{12} = (X_{12}, Y_{12}, Z_{12})$, which is the center-of-mass position of fibril 2 relative to fibril 1 in a reference frame (X, Y, Z) with Z parallel to the local director at the position of fibril 1 ($\vec{R}_{12}^{i}$ is equal to X_{12} for $i = 1$, Y_{12} for $i = 2$, Z_{12} for $i = 3$), $\hat{X}$ and $\hat{Z}$ are the unit vectors parallel to the X -axis and Z -axis respectively, $f_O(x)$ is the Onsager trial function, *i.e.*

$$f_O(x) = \frac{\alpha_N}{4\pi \sinh \alpha_N} \cosh(\alpha_N \cos x)\,, \tag{4}$$

$\dot{f}_O(x)$ is its first derivative with respect to its argument and $e_{12}^{LL'}$ is the Mayer function[12], i.e.

$$e_{12}^{LL'}\left(\vec{R}_{12}, \vec{\Omega}_1, \vec{\Omega}_2\right) = \exp\left\{-\frac{U_h\left(\vec{R}_{12}, \vec{\Omega}_1, \vec{\Omega}_2\right)}{k_B T}\right\} - 1 \tag{5}$$

where $U_h\left(\vec{R}_{12}, \vec{\Omega}_1, \vec{\Omega}_2\right)$ is the hard core interaction potential between two fibrils:

$$U_h\left(\vec{R}_{12}, \vec{\Omega}_1, \vec{\Omega}_2\right) = \begin{cases} \infty, & \text{if 1,2 overlap} \\ 0, & \text{if 1,2 do not overlap} \end{cases} \tag{6}$$

The parameter α_N in Eq. (4) is related to the degree of orientational order ($\alpha_N = 0$ in the isotropic phased and $\alpha_N > 0$ for calamitics). From α_N the order parameter S can be calculated through the following relation:

$$S = \int_0^{\pi} f_O(\theta)\ P_2(\cos\theta)\, 2\pi \sin\theta\, d\theta \tag{7}$$

where $P_2(x)$ is the second order Legendre polynomial.

Concerning L_0, according to Ref.[13], it has to be related to the deflection length $\lambda = \frac{L_p}{\alpha_N}$ rather than the bare persistence length L_p and thus we set $L_0 = \lambda = \frac{L_p}{\alpha_N}$ (see Table 1 for the experimental values of L_p used in the calculations).

As in Ref.[7] the contour length distribution $\nu(L)$ of amyloid fibrils in Eq. (2) is conveniently modelled by a log-normal distribution, *i.e.*

$$\nu(L) = \frac{A}{L\,\sigma\,\sqrt{2\pi}}\, e^{-\frac{\{\ln(L/\mathcal{L})\}^2}{2\,\sigma^2}} \tag{8}$$

where A is a normalization constant and σ and $\mathcal{L}$ are two parameters. The values of σ and $\mathcal{L}$, which we used in the calculations, are obtained from the experimental contour length distribution and they are shown in Table 1.

The generalized excluded volumes $\overline{v}_{ii}$,which enter into Eq. (2), are calculated for several values of α_N, ranging from 3.62 (S=0.4) to 50.0 (S=0.94), by employing the same procedure based on Monte Carlo integration which is discussed in the SI of Ref.[1]. In these calculations fibrils are modelled as hard cylinders of effective diameter D_{eff}, whose values, for the different fibrils investigated here, are those discussed in the main text and which are shown in Table 1.

	c_m (mg/ml)	μ_0 (10^3Da/nm)	L_c (nm)	L_p(nm)	σ	$\mathcal{L}$ (nm)	D_{eff} (nm)
BLG	28.0	5.85	461.0	1943	0.315	438.7	5.54
SCNC	24.7	11.8	246.2	3319	0.322	233.8	15.7
CCNC	8.0	7.82	317.3	1372	0.384	294.8	20.0

Table S2 *Values of the parameters c_m, μ_0, L_c (see Eq. 2), σ and $\mathcal{L}$ (see Eq. 8) and D_{eff} used in the theoretical calculations of the elastic constants for betalactoglobuline (BLG), CCNC and SCNC amyloid fibrils.*

SCNC radial cholesteric formation. Equilibrated radial cholesteric configuration has not been observed in SCNC based tactoids. However, it was possible observing droplet characterized by high volumes where the director field configuration starts to bend, suggesting that the droplet is evolving to radial cholesteric configuration[7]. The droplet diameter of these droplets approaches 200 µm, which is equal to the couvette inner diameter, and so the droplet cannot further grow in size and complete the transition at even higher volumes..

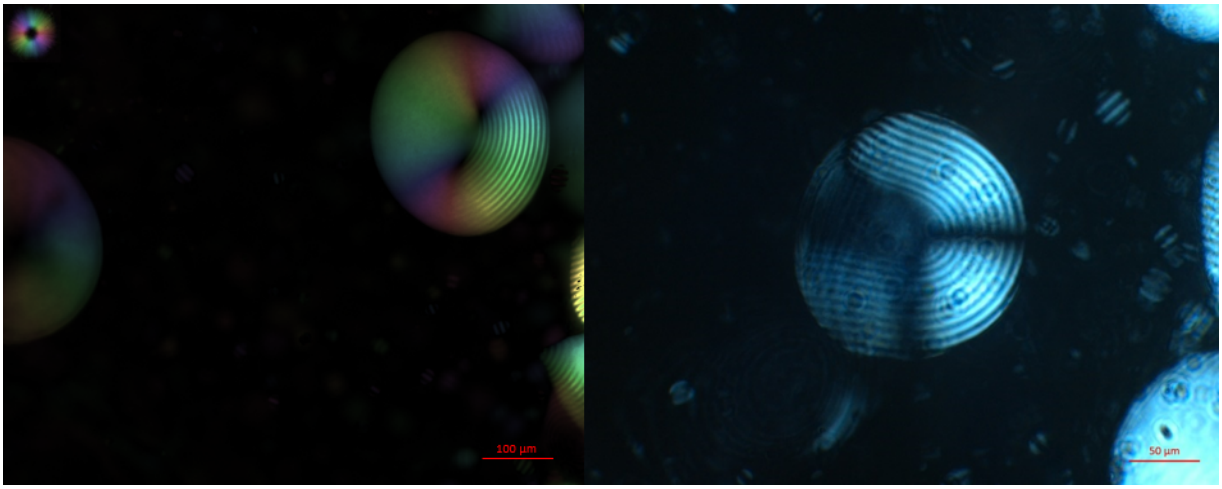

Figure S6 *Uniaxial to radial cholesteric transition. On the left, PolScope color map image of a S-CNC tactoid where the director field starts to bend, suggesting that the droplet might undergo*

radial cholesteric configuration at higher volumes. On the right, another droplet with director field bending following the interface of the droplet, viewed under cross-polarized microscope. This non-equilibrium configuration is assumed by tactoids undergoing uniaxial to radial cholesteric transition[8].

Order Parameter estimation from birefringence

Polscope analysis provides the quantitative evaluation of the optical retardance of the specimen pixel by pixel[9], allowing the estimation of the orientational order parameter S[10,11].

In particular, the optical reatardance r is equal to $r = d\Delta n$, where Δn is the specific birefringence of the specimen and d his thickness. The orientational order parameter $S = \Delta n/\Delta n_0$ where Δn_0 is the birefringence corresponding to a perfectly aligned nematic phase (S=1). The exact value of Δn_0 is experimentally elusive since the order parameter is often well below the unity for lyotropic liquid crystals. To overcome this limitation we assumed as Δn_0 the highest birefringence value measured for each system. In particular, these strongly birefringence domains were found at the bulk nematic phase in macroscopically phase separated systems (BLG and SCNC), or at the edge of the couvette (for CCNC liquid-glue interface) where slow evaporation induces strong fibril alignment.

The order parameter was calculated for several tactoids by measuring thickness and specific retardance at the center of each tactoid in the same couvette used for the other experiments (inner D = 200 μm). Figure S4 show the order parameter plotted as function of tactoid volume for tactoids with different director field configurations.

The average order parameter measured in BLG cholesteric tactoids is equal to 0.54, which is in good agreement with previously reported value of 0.49±0.03, extracted with fluorescence analysis[7]. In case of CCNC and SCNC the average order parameter measured in cholesteric tactoids is equal to 0.58±0.06 and 0.89±0.06 respectively.

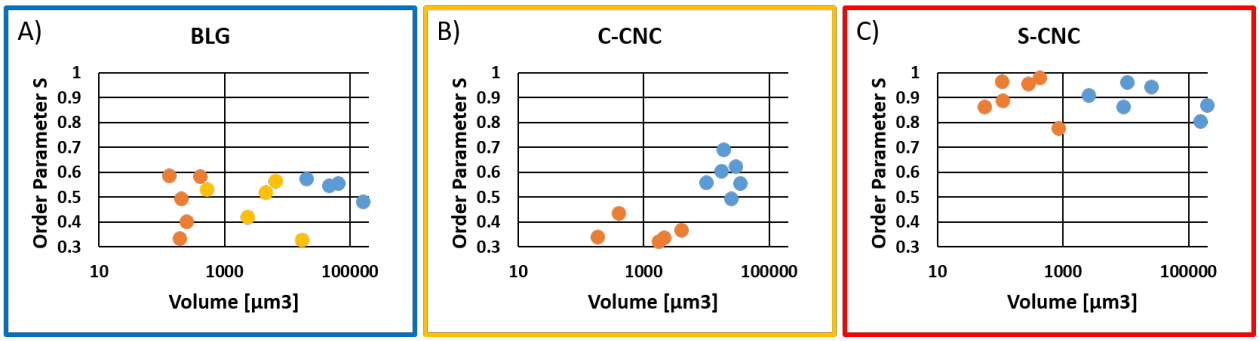

Figure S7 *Order Parameter estimation from birefringence measurements: Estimation of the order parameter S for tactoids of BLG (A), CCNC (B) and SCNC (C). The points in orange correspond to homogeneous tactoids, in yellow bipolar and blue uniaxial cholesteric. The average order parameter S in uniaxial cholesteric droplets for the three system is equal to 0.54±0.03 for BLG, 0.58±0.06 for CCNC and 0.89±0.06 for SCNC.*

References

1. Vroege, G. J. & Odijk, T. Elastic moduli of a nematic liquid-crystalline solution of polyelectrolytes. *J. Chem. Phys.* **87**, 4223–4232 (1987).

2. Nyström, G., Arcari, M. & Mezzenga, R. Confinement-induced liquid crystalline transitions in amyloid fibril cholesteric tactoids. *Nat. Nanotechnol.* **13**, 330–336 (2018).

3. Nyström, G., Arcari, M., Adamcik, J., Usov, I. & Mezzenga, R. Nanocellulose Fragmentation Mechanisms and Inversion of Chirality from the Single Particle to the Cholesteric Phase. *ACS Nano* **12**, 5141–5148 (2018).

4. Usov, I. *et al.* Understanding nanocellulose chirality and structure-properties relationship at the single fibril level. *Nat. Commun.* **6**, 7564 (2015).

5. Adamcik, J. *et al.* Understanding amyloid aggregation by statistical analysis of atomic force microscopy images. *Nat. Nanotechnol.* **5**, 423–428 (2010).

6. Nyström, G., Arcari, M., Adamcik, J., Usov, I. & Mezzenga, R. Nanocellulose Fragmentation Mechanisms and Inversion of Chirality from the Single Particle to the Cholesteric Phase. *ACS Nano* **12**, 5141–5148 (2018).

7. Bagnani, M., Nyström, G., De Michele, C. & Mezzenga, R. Amyloid Fibrils Length Controls Shape and Structure of Nematic and Cholesteric Tactoids. *ACS Nano* **13**, 591–600 (2019).

8. Bagnani, M., Azzari, P., Assenza, S. & Mezzenga, R. Six-fold director field configuration in amyloid nematic and cholesteric phases. *Sci. Rep.* **9**, (2019).

9. Oldenbourg, R., Salmon, E. D. & Tran, P. T. Birefringence of single and bundled

microtubules. in *Biophysical Journal* **74**, 645–654 (Biophysical Society, 1998).

10. Viamontes, J., Narayanan, S., Sandy, A. R. & Tang, J. X. Orientational order parameter of the nematic liquid crystalline phase of F -actin. *Phys. Rev. E - Stat. Nonlinear, Soft Matter Phys.* **73**, 061901 (2006).

11. Gentry, B., Smith, D. & Käs, J. Buckling-induced zebra stripe patterns in nematic F-actin. *Phys. Rev. E - Stat. Nonlinear, Soft Matter Phys.* **79**, (2009).

12. Romani, E., Ferrarini, A. & De Michele, C. Elastic Constants of Chromonic Liquid Crystals. *Macromolecules* **51**, 5409–5419 (2018).

13. Odijk, T. Elastic constants of nematic solutions of rod-like and semi-flexible polymers. *Liq. Cryst.* **1**, 553–559 (1986).